

# Highly relativistic spinning particle starting near $r_{ph}^{(-)}$ in a Kerr field

Roman Plyatsko, Oleksandr Stefanyshyn, and Mykola Fenyk  
*Pidstryhach Institute for Applied Problems in Mechanics and Mathematics*  
*Ukrainian National Academy of Sciences, 3-b Naukova Str.,*  
*Lviv, 79060, Ukraine*  
 (Dated: November 15, 2018)

Using the Mathisson-Papapetrou-Dixon (MPD) equations, we investigate the trajectories of a spinning particle starting near  $r_{ph}^{(-)}$  in a Kerr field and moving with the velocity close to the velocity of light ( $r_{ph}^{(-)}$  is the Boyer-Lindquist radial coordinate of the counter-rotation circular photon orbits). First, as a partial case of these trajectories, we consider the equatorial circular orbit with  $r = r_{ph}^{(-)}$ . This orbit is described by the solution that is common for the rigorous MPD equations and their linear spin approximation. Then different cases of the nonequatorial motions are computed and illustrated by the typical figures. All these orbits exhibit the effects of the significant gravitational repulsion that are caused by the spin-gravity interaction. Possible applications in astrophysics are discussed.

PACS numbers: 04.20.-q, 95.30.Sf

## I. INTRODUCTION

The geodesics in a Kerr metric are considered in the classical books on general relativity [1–3]. Some recent papers are devoted to more detailed study of geodesics on Kerr's black hole with the aim to elucidate the mechanism of jet formation [4], and to analyze the possibility of particle acceleration to arbitrary high energy [5]. The complete sets of analytic solutions of the geodesic equation in axially symmetric space-time are given in [6]. However, the description of particle motion by geodesics is restricted to a spinless particle. The motion of a spinning test particle is described by the Mathisson-Papapetrou-Dixon equations [7–9]:

$$\frac{D}{ds} \left( mu^\lambda + u_\mu \frac{DS^{\lambda\mu}}{ds} \right) = -\frac{1}{2} u^\pi S^{\rho\sigma} R_{\pi\rho\sigma}^\lambda, \quad (1)$$

$$\frac{DS^{\mu\nu}}{ds} + u^\mu u_\sigma \frac{DS^{\nu\sigma}}{ds} - u^\nu u_\sigma \frac{DS^{\mu\sigma}}{ds} = 0, \quad (2)$$

where  $u^\lambda \equiv dx^\lambda/ds$  is the particle's 4-velocity,  $S^{\mu\nu}$  is the tensor of spin,  $m$  and  $D/ds$  are, respectively, the mass and the covariant derivative with respect to the particle's proper time  $s$ ;  $R_{\pi\rho\sigma}^\lambda$  is the Riemann curvature tensor (units  $c = G = 1$  are used). It is necessary to add a supplementary condition to Eqs. (1), (2) in order to choose an appropriate trajectory of the particle's center of mass. Most often the conditions

$$S^{\lambda\nu} u_\nu = 0 \quad (3)$$

and

$$S^{\lambda\nu} P_\nu = 0 \quad (4)$$

are used, where

$$P^\nu = mu^\nu + u_\lambda \frac{DS^{\nu\lambda}}{ds} \quad (5)$$

is the 4-momentum. In practice, the condition for a spinning test particle

$$\frac{|S_0|}{mr} \equiv \varepsilon \ll 1 \quad (6)$$

must be taken into account [10], where  $|S_0| = \text{const}$  is the absolute value of spin,  $r$  is the coordinate distance of the particle from the massive body.

After [7–9], Eqs. (1), (2) were obtained in many papers by different approaches [11]. Also, this subject is of importance in some recent publications [12].

In general, the solutions of Eqs. (1), (2) under conditions (3) and (4) are different. However, in the post-Newtonian approximation these solutions coincide with high accuracy [13], just as in the case if the spin effects can be described by a convergent in spin series, as some corrections to the corresponding geodesic expressions [14]. Therefore, instead of rigorous MPD Eqs. (1) their linear spin approximation

$$m \frac{D}{ds} u^\lambda = -\frac{1}{2} u^\pi S^{\rho\sigma} R_{\pi\rho\sigma}^\lambda \quad (7)$$

is often considered. In this approximation condition (4) coincides with (3).

The effect of spin on the particle's motion in Kerr's field has been studied since the 1970s [10,15,16]. In the past 10–12 years this subject gives rise to renewed interest [17–22], particularly in the context of investigations of the possible chaotic motions [17,19]. Also, these references provide a good introduction concerning the MPD equations.

The purpose of this paper is to investigate more carefully the world lines and trajectories of a spinning particle moving relative to a Kerr source with the velocity close to the velocity of light. We focus on the circular and close to circular orbits, because just on these orbits one

can expect the significant effects of the spin-gravity interaction [10,23–25]. Indeed, these orbits are of interest in the context of investigations of the nongeodesic synchrotron electromagnetic radiation of highly relativistic protons and electrons near black holes. Besides, it is known that the highly relativistic circular orbits of a spinless particle are of importance in the classification of all possible geodesic orbits in a Kerr spacetime. Naturally, the circular highly relativistic orbits of a spinning particle are of importance in the classification of all possible significantly nongeodesic orbits in this spacetime as well. Also, these orbits are exclusive in the sense that they are described by the strict analytical solutions of the MPD equations. The main features of the spin-gravity interaction that are revealed on the circular and close to circular orbits will be a good reference to further investigations of most general motions of a spinning particle in a Kerr spacetime.

We stress that MPD equations are the classical limit of the general relativistic Dirac equation [26], new results in this context are presented in [27]. Therefore, highly relativistic solutions of the MPD equations stimulate the corresponding investigations of the fermion's interaction with the strong gravitational field.

The paper is organized as follows. Sec. 2 deals with the relationships following from the MPD equations for the highly relativistic equatorial circular orbits of a spinning particle in Kerr's field, in the Boyer-Lindquist coordinates. The linear spin MPD equations for any motions of a spinning particle are considered in Sec. 3. The results of computer integration of these equations for some significantly nongeodesic motions are presented in Sec. 4. We conclude in Sec. 5.

Following [3], in this paper  $r_{ph}^{(-)}$  notes the radial coordinate of the photon circular orbits in the case of the counter-rotation.

## II. HIGHLY RELATIVISTIC EQUATORIAL CIRCULAR ORBITS OF SPINNING PARTICLES IN A KERR FIELD ACCORDING TO APPROXIMATE AND RIGOROUS MPD EQUATIONS

In practical calculations it is convenient to represent the MPD equations through the spin 3-vector  $S_i$ , instead of the 4-tensor  $S^{\mu\nu}$ , where by definition

$$S_i = \frac{1}{2}\sqrt{-g}\varepsilon_{ikl}S^{kl}, \quad (8)$$

where  $g$  is the determinant of  $g_{\mu\nu}$ ,  $\varepsilon_{ikl}$  is the Levi-Civita symbol (here and in the following, latin indices run 1, 2, 3, and greek indices 1, 2, 3, 4, unless otherwise specified). Then Eqs. (2) can be written as [23]

$$u_4\dot{S}_i - \dot{u}_4S_i + 2(\dot{u}_{[4}u_{i]} - u^\pi u_\rho \Gamma_{\pi[4}^\rho u_{i]})S_k u^k + 2S_n \Gamma_{\pi[4}^n u_{i]} u^\pi = 0, \quad (9)$$

where a dot denotes differentiation with respect to the proper time  $s$ , and square brackets denote antisymmetrization of indices;  $\Gamma_{\beta\gamma}^\alpha$  are the Christoffel symbols. Eq. (7) in terms of  $S_i$  is

$$m(\dot{u}^\lambda + \Gamma_{\alpha\beta}^\lambda u^\alpha u^\beta) + \frac{u^\pi}{2u_4\sqrt{-g}}(u_4 R_{\pi ik}^\lambda + 2u_i R_{\pi k4}^\lambda)\varepsilon^{ikl}S_l = 0. \quad (10)$$

In many papers the 4-vector of spin  $s_\lambda$  is considered, where

$$s_\lambda = \frac{1}{2}\sqrt{-g}\varepsilon_{\lambda\mu\nu\sigma}u^\mu S^{\nu\sigma}.$$

The following relationship holds:

$$S_i = u_i s_4 - u_4 s_i.$$

Let us consider Eqs. (9), (10) for the Kerr metric using the Boyer-Lindquist coordinates  $x^1 = r$ ,  $x^2 = \theta$ ,  $x^3 = \varphi$ ,  $x^4 = t$ . Then the nonzero components of  $g_{\mu\nu}$  are

$$g_{11} = -\frac{\rho^2}{\Delta}, \quad g_{22} = -\rho^2, \\ g_{33} = -\left(r^2 + a^2 + \frac{2Mra^2}{\rho^2}\sin^2\theta\right)\sin^2\theta, \\ g_{34} = \frac{2Mra}{\rho^2}\sin^2\theta, \quad g_{44} = 1 - \frac{2Mr}{\rho^2}, \quad (11)$$

where

$$\rho^2 = r^2 + a^2 \cos^2\theta, \quad \Delta = r^2 - 2Mr + a^2, \quad 0 \leq \theta \leq \pi.$$

[In the following we shall put  $a \geq 0$ , without any loss in generality; the metric signature is  $---+$ .] It is easy to check that three equations from (9) have a partial solution with  $\theta = \pi/2$ ,  $S_1 \equiv S_r = 0$ ,  $S_3 \equiv S_\varphi = 0$  and the relationship for the nonzero component of the spin 3-vector  $S_2 \equiv S_\theta = 0$  is

$$S_2 = ru_4 S_0, \quad (12)$$

where  $S_0$  is the constant of integration. The physical meaning of this constant is the same as in the general integral of the MPD equations [15]

$$S_0^2 = \frac{1}{2}S_{\mu\nu}S^{\mu\nu}. \quad (13)$$

We stress that relationship (12) is valid for any equatorial motions ( $\theta = \pi/2$ ), with the spin orthogonal to the motion plane ( $S_i u^i = 0$ ).

The possible equatorial orbits of a spinning particle are described by Eq. (10). First, we shall consider the case of the circular orbits with

$$u^1 = 0, \quad u^2 = 0, \quad u^3 = \text{const} \neq 0, \quad u^4 = \text{const} \neq 0. \quad (14)$$

Investigating the conditions of existence of the equatorial circular orbits for a spinning particle in Kerr's field we use Eqs. (10), (12), and  $u^\mu u_\mu = 1$ . It is known that from the geodesic equations in this field, the algebraic relationship that follows determines the dependence of the velocity of a spinless particle on the radial coordinate  $r$  of the equatorial circular orbit. Similarly, from the first equation of set (10) using Eq. (14) we obtain the relationship for the equatorial circular orbits of a spinning particle in Kerr's field as follows:

$$\Gamma_{33}^1 (u^3)^2 + 2\Gamma_{34}^1 u^3 u^4 + \Gamma_{44}^1 (u^4)^2 - \frac{\Delta^2 S_2}{r^4 m u_4} \\ \times [(u^3)^2 R_{113}^4 + u^3 u^4 (R_{114}^4 - R_{113}^3) - (u^4)^2 R_{114}^3] = 0. \quad (15)$$

[By Eq. (14) other equations of set (10) are automatically satisfied.] Taking into account Eq. (12) and the explicit expressions for  $\Gamma_{\mu\nu}^\lambda$  and  $R_{\pi\rho\sigma}^\lambda$  (see, e.g., [18]) from Eq. (15) we obtain

$$(Ma^2 - r^3)(u^3)^2 - 2Ma u^3 u^4 + M(u^4)^2 - \frac{3MS_0}{mr^2} \\ \times [a^2(r^2 + a^2)(u^3)^2 - (r^2 + 2a^2)u^3 u^4 + a(u^4)^2] = 0. \quad (16)$$

The 4-velocity component  $u^4$  can be expressed through  $u^3$  from the condition  $u^\mu u_\mu = 1$  as follows:

$$u^4 = -\frac{g_{34}u^3}{g_{44}} + \sqrt{\frac{g_{34}^2 - g_{33}g_{44}}{g_{44}^2}(u^3)^2 + \frac{1}{g_{44}}} \quad (17)$$

(just the sign "+" at the radical in Eq. (17) ensures the positive value of  $u^4$ ). Inserting expression (17) into Eq. (16) and eliminating the radical by raising to the second power we get

$$(u^3)^4 (r^5 [r(r-3M)^2 - 4Ma^2] + 12\epsilon Mar^4 \Delta - 9\epsilon^2 M^2 r^4 \Delta) \\ + (u^3)^2 (-2Mr^4(r-3M) + 6\epsilon Mar^3(r-3M) \\ - 9\epsilon^2 M^2 r^3(r-2M)) + M^2(r-3\epsilon a)^2 = 0, \quad (18)$$

where, as in Eq. (6),  $\epsilon = |S_0|/mr$ . Without any loss in generality we put  $S_0 > 0$ , then by Eq. (12)  $S_2 > 0$ .

So, the particle's angular velocity  $\dot{\varphi} = u^3$  on the circular orbit with the radial coordinate  $r$  must satisfy Eq. (18).

Let us show that Eq. (18) provides known solutions. In the partial case of a spinless particle ( $\epsilon = 0$ ) from Eq. (18) we have

$$(u^3)^2 = \frac{Mr(r-3M) + 2Ma\sqrt{Mr}}{r^2[r(r-3M)^2 - 4Ma^2]}. \quad (19)$$

It follows from Eq. (19) that the velocity of such a particle on the circular orbit is highly relativistic if the expression  $r(r-3M)^2 - 4Ma^2$  is close to 0. This fact is known from the analysis of the geodesic orbits in a Kerr field, as well as that just the roots of the equation

$$r(r-3M)^2 - 4Ma^2 = 0$$

determine the values of  $r$  for the photon orbits.

If  $\epsilon \neq 0$  and the absolute value of the expression  $r^5[r(r-3M)^2 - 4Ma^2]$  in the factor of  $(u^3)^4$  in Eq. (18) is much greater than  $12\epsilon Mar^4 \Delta - 9\epsilon^2 M^2 r^4 \Delta$ , then it is easy to verify that the corresponding roots of Eq. (18) describe the circular orbits with the angular velocity which is close to the angular velocity of the corresponding geodesic orbits due to  $\epsilon \ll 1$ . More exactly, in this case we have

$$|u^3| = \sqrt{\frac{Mr(r-3M) + 2Ma\sqrt{Mr}}{r^2[r(r-3M)^2 - 4Ma^2]}}(1 + O(\epsilon)), \quad (20)$$

where the main term is equal to the square root of the right-hand side of Eq. (19).

Now we point out a case of interest with  $\epsilon \neq 0$  that is not described in the literature. Namely, it is not difficult to calculate that for  $\epsilon \neq 0$  Eqs. (16), (18) have the solutions which describe the highly relativistic circular orbits with the values of  $r$  that is equal or close to  $r_{ph}^{(-)}$ , i.e., to the radial coordinate of the counter-rotation photon circular orbits. For example, in the case of the maximum Kerr field ( $a = M$ ) the orbits with  $r = 4M(1 + \delta)$ , where  $|\delta| \ll 1$ , are highly relativistic, both for positive and negative  $\delta$ . If  $|\delta| \ll \epsilon$ , according to Eqs. (16), (18) the values of  $u^3$  on these orbits are determined by the expression

$$u^3 = -\frac{1}{3M\sqrt{6\epsilon(1+4\delta/3\epsilon)}}(1 + O(\epsilon)). \quad (21)$$

[The choice of the sign in Eq. (21),  $u^3 < 0$ , is dictated by the necessity to satisfy both Eq. (18) and (16); Eq. (18), as compared to (16), has additional roots because of the operation of raising to the second power.] Similarly as in the case of Eq. (20), it is easy to check that if  $\epsilon \ll |\delta|$  it follows from Eqs. (16), (18) the expression for  $u^3$  which in the main term coincides with the known analytic solution for the corresponding geodesic circular orbit.

It follows from Eqs. (16), (18) at  $r = r_{ph}^{(-)}$  for any  $0 \leq a \leq M$  that

$$u^3 = -\frac{2(M/r_{ph}^{(-)})^{3/4}}{\sqrt{3\epsilon}(r_{ph}^{(-)} - M)}(1 + O(\epsilon)). \quad (22)$$

It is known from the geodesic equations that the values of  $r_{ph}^{(-)}$  increase monotonically from  $3M$  at  $a = 0$  to  $4M$  at  $a = M$ .

Thus, according to Eq. (22) the expression for the angular velocity  $\dot{\varphi} = u^3$  in the main term is proportional

to  $1/\sqrt{\varepsilon}$ , whereas the angular velocity in Eq. (20) at  $r = r_{ph}^{(-)}(1 + \delta)$ ,  $0 < \delta \ll 1$  is proportional to  $1/\sqrt{\delta}$ . Further details appear below in this Sec.

Using Eq. (22) we can estimate the value of the Lorentz  $\gamma$ -factor, corresponding to the 4-velocity component  $u^3$ , for different  $a$ . More exactly, we shall calculate the Lorentz  $\gamma$ -factor from the point of view of an observer which is at rest relative to a Kerr mass. According to the general expression for the 3-velocity components  $v^i$  we write [1]

$$v^i = \frac{dx^i}{\sqrt{g_{44}}} \left( dt + \frac{g_{4i}}{g_{44}} dx^i \right)^{-1} \quad (23)$$

and for the second power of the velocity absolute value  $|v|^2$  we have

$$|v|^2 = v_i v^i = \gamma_{ij} v^i v^j, \quad (24)$$

where  $\gamma_{ij}$  is the 3-space metric tensor. The relationship between  $\gamma_{ij}$  and  $g_{\mu\nu}$  is as follows:

$$\gamma_{ij} = g_{ij} + \frac{g_{4i} g_{4j}}{g_{44}}. \quad (25)$$

For the circular motions we have  $v^1 = 0$ ,  $v^2 = 0$ , and according to Eq. (23)

$$v^3 = \frac{dx^3}{\sqrt{g_{44}}} \left( dt + \frac{g_{4i}}{g_{44}} dx^i \right)^{-1} = \frac{u^3}{\sqrt{g_{44}}} \left( u^4 + \frac{g_{43}}{g_{44}} u^3 \right)^{-1}. \quad (26)$$

By Eqs. (24)-(26) and the condition  $u^\mu u_\mu = 1$ , for the  $\gamma$ -factor we write

$$\gamma = \frac{1}{\sqrt{1 - v^2}} = \sqrt{(u^3)^2 \left( -g_{33} + \frac{g_{43}^2}{g_{44}} \right) + 1}. \quad (27)$$

Inserting the value  $u^3$  from Eq. (22) into Eq. (27) we find in the corresponding spin approximation

$$\gamma = \frac{1}{\sqrt{3\varepsilon}} \left( \frac{M}{r_{ph}^{(-)}} \right)^{-1/4} \left( 1 - \frac{2M}{r_{ph}^{(-)}} \right)^{-1/2}. \quad (28)$$

It follows from Eq. (28) that  $\gamma^2 \gg 1$ , i.e., the under consideration circular motions are highly relativistic. Fig. 1 shows the dependence  $\gamma/\gamma_0$  on  $r_{ph}^{(-)}/M$ , where  $\gamma_0$  is the  $\gamma$ -factor for  $r_{ph}^{(-)} = 3M$ , that is, at  $a = 0$ .

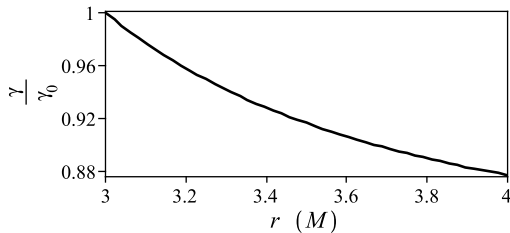


FIG. 1. Ratio  $\gamma$ -factor at different  $a$ , from  $0 < a \leq M$ , to  $\gamma$ -factor at  $a = 0$  vs. radial coordinate.

It is known that the important characteristic of the particle's motion in the Kerr spacetime are its energy and angular momentum. Let us estimate the conserved values of the energy  $E$  and angular momentum  $J$  of a spinning particle on the above considered highly relativistic circular orbits with Eqs. (21), (22). The expressions for these quantities are [16,28]

$$E = mu_4 + g_{34} u_\mu \frac{DS^{3\mu}}{ds} + g_{44} u_\mu \frac{DS^{4\mu}}{ds} + \frac{1}{2} S^{\mu\nu} g_{\nu 4, \mu}, \quad (29)$$

$$J = -mu_3 - g_{33} u_\mu \frac{DS^{3\mu}}{ds} - g_{34} u_\mu \frac{DS^{4\mu}}{ds} - \frac{1}{2} S^{\mu\nu} g_{\nu 3, \mu}. \quad (30)$$

By Eqs. (21), (29) for  $r = 4M(1 + \delta)$ ,  $|\delta| \ll \varepsilon$  we obtain

$$E_{spin} = \frac{m}{\sqrt{6\varepsilon}}. \quad (31)$$

The energy of a spinless particle on the geodesic circular orbit with  $r = 4M(1 + \delta)$ ,  $0 < \delta \ll 1$  for  $a = M$  is equal to

$$E_{geod} = \frac{3m}{2\sqrt{10\delta}}. \quad (32)$$

It follows from Eqs. (31), (32) that

$$E_{spin}^2/m^2 \gg 1, \quad E_{geod}^2/m^2 \gg 1. \quad (33)$$

At the same time according to (31), (32) for  $0 < \delta \ll \varepsilon$  we have

$$E_{spin}^2/E_{geod}^2 = \frac{20\delta}{27\varepsilon} \ll 1. \quad (34)$$

That is, the values of energy of the spinning and spinless particles on the highly relativistic circular orbits with the same  $r = 4M(1 + \delta)$  in the maximal Kerr field can differ significantly. It is easy to show that similar situation takes place for all values  $0 \leq a \leq M$  with  $r = r_{ph}^{(-)}(1 + \delta)$ . In addition, one can estimate for these circular orbits that according to Eq. (30)  $J_{spin}^2/J_{geod}^2 \ll 1$ .

As a result, the relationships  $E_{spin}^2/E_{geod}^2 \ll 1$  and  $J_{spin}^2/J_{geod}^2 \ll 1$  following from Eqs. (29), (30) show clearly that the corresponding solutions of the MPD equations cannot be obtained in the framework of the analytic perturbation approach to the dynamics of a classical spinning particle developed in [20–22].

We stress that in this Sec. above we have considered the new highly relativistic circular solutions of the approximate MPD Eqs. (2), (7). Let us show that these solutions satisfy the rigorous MPD Eqs. (1), (2). Indeed, it follows from Eqs. (1) that their terms, which were neglected in Eqs. (7), in the case of the circular equatorial motions are presented in the first Eq. of set (1) only. In metric (11) these terms can be written as

$$c_1(u^3)^4 + c_2(u^4)^4 + c_3(u^3)^3 u^4 + c_4(u^3)^2 (u^3)^2 + c_5 u^3 (u^4)^3, \quad (35)$$

where

$$c_1 = S_0 \Delta \frac{Ma}{r^7} (3r^2 + a^2)(r^3 - Ma^2),$$

$$c_2 = -S_0 \Delta \frac{M^2 a}{r^7} \left( 1 - \frac{2M}{r} \right),$$

$$c_3 = S_0 \frac{\Delta}{r^7} [r^5(r - 3M)(r^3 - 3Ma^2) + 4M^2 a^4],$$

$$c_4 = S_0 \Delta \frac{Ma}{r^7} \left( 3r^3 - 11Mr^2 - 6Ma^2 + \frac{2M^2 a^2}{r} \right),$$

$$c_5 = -S_0 \frac{M\Delta}{r^7} \left( r^3 - 3Mr^2 - 4Ma^2 + \frac{4M^2 a^2}{r} \right). \quad (36)$$

First, we point out that according to Eq. (36) in the case of a Schwarzschild's field for the circular orbit with  $r = 3M$  the all coefficients  $c_i$  are equal to 0. Therefore, in this case expression (35) is equal to 0 identically, independently on the explicit expressions for  $u^3$ ,  $u^4$ . It means that the highly relativistic circular orbit of a spinning particle with  $r = 3M$  in a Schwarzschild's field is a common strict solution both of the approximate MPD equations (2), (7) and the rigorous MPD equations (1), (2). Second, it is not difficult to check that applying Eqs. (17), (22) to expression (35) at  $a \neq 0$  yields 0 in the main terms, i.e., within the accuracy of order  $\varepsilon$ .

Thus, in this Sec. we dealt with new partial solutions of the MPD equations in a Kerr spacetime with Eqs. (12), (14), (22). All highly relativistic orbits of a spinning particle described by these solutions are circular and located in the space region with  $r = r_{ph}^{(-)}(1 + \delta)$ ,  $|\delta| \ll 1$ . To study highly relativistic orbits beyond this region it is necessary to carry out the corresponding computer calculations. It is an aim of Secs. 3 and 4.

### III. EQUATIONS (7), (9) FOR ANY MOTIONS IN A KERR FIELD

Now the point of interesting is the noncircular highly relativistic motions of a spinning particle that starts near  $r_{ph}^{(-)}$  in a Kerr field. In particular, we shall consider the effect of the 3-vector  $S_i$  inclination to the equatorial plane  $\theta = \pi/2$  on the particle's trajectory. In this case Eqs. (9) cannot be integrated separately from Eqs. (7). For computer integration, it is necessary to write the explicit form of Eqs. (7), (9) in metric (11). It is convenient to use the dimensionless quantities  $y_i$ , where by definition

$$y_1 = \frac{r}{M}, \quad y_2 = \theta, \quad y_3 = \varphi, \quad y_4 = \frac{t}{M},$$

$$y_5 = u^1, \quad y_6 = Mu^2, \quad y_7 = Mu^3, \quad y_8 = u^4,$$

$$y_9 = \frac{S_1}{mM}, \quad y_{10} = \frac{S_2}{mM^2}, \quad y_{11} = \frac{S_3}{mM^2}, \quad (37)$$

and

$$x = \frac{s}{M}, \quad \varepsilon_0 = \frac{|S_0|}{mM} \quad (38)$$

(in contrast to  $\varepsilon$  from (6), that depends on  $r$ , here  $\varepsilon_0$  is defined to be *const*). Then it follows from Eqs. (7), (9) the set of 11 first-order differential equations

$$\dot{y}_1 = y_5, \quad \dot{y}_2 = y_6, \quad \dot{y}_3 = y_7, \quad \dot{y}_4 = y_8,$$

$$\dot{y}_5 = A_1, \quad \dot{y}_6 = A_2, \quad \dot{y}_7 = A_3, \quad \dot{y}_8 = A_4,$$

$$\dot{y}_9 = A_5, \quad \dot{y}_{10} = A_6, \quad \dot{y}_{11} = A_7, \quad (39)$$

where a dot denotes differentiation with respect to  $x$ , and  $A_j$  ( $j = 1, \dots, 7$ ) are some functions which depend on  $y_i$ . Because the expressions for  $A_i$  in general case of any  $a$  are too lengthy, here we write  $A_i$  for the much simpler case  $a = 0$ :

$$A_1 = \frac{y_5^2}{y_1^2} q + \left( y_1 y_6^2 + y_1 y_7^2 \sin^2 y_2 - \frac{y_8^2}{y_1^2} \right) q^{-1}$$

$$+ \frac{3}{y_1^3 \sin y_2} (y_7 y_{10} \sin^2 y_2 - y_6 y_{11}),$$

$$A_2 = y_7^2 \cos y_2 \sin y_2 - \frac{2y_5 y_6}{y_1} - \frac{3y_7 y_9}{y_1^3} \sin y_2,$$

$$A_3 = -\frac{2y_5 y_7}{y_1} - 2y_6 y_7 \cot y_2 + \frac{3y_6 y_9}{y_1^3 \sin y_2},$$

$$A_4 = -\frac{2y_5 y_8}{y_1^2} q - \frac{3y_5}{y_1^3 y_8 \sin y_2} q^2$$

$$\times (y_7 y_{10} \sin^2 y_2 - y_6 y_{11}),$$

$$A_5 = \frac{2}{y_1^2} y_5 y_9 q + \frac{y_6 y_{10}}{y_1} + \frac{y_7 y_{11}}{y_1}$$

$$- (y_5 y_9 + y_6 y_{10} + y_7 y_{11}) [A_1 q$$

$$- \frac{y_5}{y_8} A_4 q - 3 \frac{y_5^2}{y_1^2} q^2$$

$$- y_1 y_6^2 - y_1 y_7^2 \sin^2 y_2 + \frac{y_8^2}{y_1^2}] + \frac{y_9}{y_8} A_4,$$

$$\begin{aligned}
A_6 &= -y_1 y_6 y_9 \left(1 - \frac{3}{y_1}\right) + \frac{y_5 y_{10}}{y_1} \left(\frac{2}{y_1} q + 1\right) \\
&+ y_7 y_{11} \cot y_2 + \frac{y_{10}}{y_8} A_4 - (y_5 y_9 + y_6 y_{10} + y_7 y_{11}) \\
&\times [y_1^2 A_2 - \frac{y_1^2 y_6}{y_8} A_4 + 2y_5 y_6 (y_1 - q) \\
&\quad - y_1^2 y_7^2 \cos y_2 \sin y_2], \\
A_7 &= \frac{y_5 y_{11}}{y_1} \left(\frac{2}{y_1} q + 1\right) \\
&- y_1 y_7 y_9 \left(1 - \frac{3}{y_1}\right) \sin^2 y_2 - y_6 y_{11} \cot y_2 \\
&- y_7 y_{10} \cos y_2 \sin y_2 - (y_5 y_9 + y_6 y_{10} + y_7 y_{11}) [A_3 y_1^2 \sin^2 y_2 \\
&\quad - A_4 \frac{y_1^2 y_7}{y_8} \sin^2 y_2 + 2y_5 y_7 (y_1 - q) \sin^2 y_2 \\
&\quad + 2y_1^2 y_6 y_7 \cos y_2 \sin y_2] + \frac{y_{11}}{y_8} A_4, \tag{40}
\end{aligned}$$

where

$$q \equiv \left(1 - \frac{2}{y_1}\right)^{-1}.$$

According to Eqs. (13), (38) the expression for  $\varepsilon_0^2$  can be written as

$$\begin{aligned}
\varepsilon_0^2 &= \frac{y_9^2}{y_8^2} q(1 + qy_5^2) + \frac{y_{10}^2}{y_1^2 y_8^2} q^2(1 + y_1^2 y_6^2) \\
&\quad + \frac{y_{11}^2 q^2}{y_1^2 y_8^2 \sin^2 y_2} (1 + y_1^2 y_7^2 \sin^2 y_2) \\
&+ \frac{2q^2}{y_8^2} (y_5 y_6 y_9 y_{10} + y_5 y_7 y_9 y_{11} + y_6 y_7 y_{10} y_{11}). \tag{41}
\end{aligned}$$

Eqs. (39)–(41) are aimed at computer integration.

#### IV. NUMERICAL RESULTS

We present here the results of computer integration of Eqs. (39) with (40), (41). All plots below are restricted to the domains of validity of the linear spin approximation. That is, in these domains the neglected terms of the rigorous MPD equations are much less than the linear spin

terms. We monitor errors of computing using the conserved quantities: the absolute value of spin, the energy and angular momentum (see Eqs. (13), (29), (30)).

Figs. 2–9 correspond to the case of Schwarzschild's field. All plots start with the same initial values of the coordinates  $x^1 = r$ ,  $x^2 = \theta$ ,  $x^3 = \varphi$ ,  $x^4 = t$ , namely, at  $3M$ ,  $90^\circ$ ,  $0^\circ$ , and 0 correspondingly. We do not vary the initial values of the 4-velocity components  $u^2$  and  $u^3$  as well. More exactly, we put  $u^2 = 0$  and

$$u^3 = -\frac{1}{3M\sqrt{2}} \sqrt{-1 + \frac{\sqrt{12 + \varepsilon_0^2}}{\varepsilon_0}}, \tag{42}$$

where expression (42) is the solution of Eq. (18) at  $a = 0$ , rigorous in  $\varepsilon_0$ . That is, the initial values of  $u^2$  and  $u^3$  are the same as for the equatorial circular orbit with  $r = 3M$  (it is easy to check that expression (42) coincides with (22) in the corresponding spin approximation). However, we vary the initial inclination angle of the spin 3-vector to the plane  $\theta = 90^\circ$ , without change of the absolute value of spin (Figs. 2–6), and add the small perturbation by the radial velocity (Figs. 7–9). Without any loss in generality we put  $S_1 > 0$ . For comparison, we present the corresponding solutions of the geodesic equations that start with the same initial values of the coordinates and velocity as the solutions of the equations for a spinning particle. In all cases as a typical value we put  $\varepsilon_0 = 10^{-4}$ .

Figs. 2–9 let us compare the world lines and trajectories of the spinning and spinless particles in Schwarzschild's field. Figs. 2, 6, 7, 9 exhibit the significant repulsive effects of the spin-gravity interaction on the spinning particle. Due to the repulsive action the spinning particle falls on the horizon surface during longer time as compared to the spinless particle (Fig. 2). Moreover, according to Figs. 6, 9 the considerable space separation takes place within a short time, i.e., within the time of the spinless particle's fall on the horizon.

The point of interest is the phenomenon when a spinning particle orbits below the equatorial plane for some revolutions, Figs. 3, 8 (we recall that according to the geodesic equations similar situation is impossible for a spinless particle). It is easy to calculate that for  $S_1 < 0$  a spinning particle can orbit above the equatorial plane.

We stress that all graphs in Figs. 2–9 are interrupted beyond the domain of validity of the linear spin approximation. By Figs. 3, 4, within the time of this approximation validity, the period of the  $\theta$ -oscillation coincides with the period of the particle's revolution by  $\varphi$ . Whereas on this interval the value of the spin component  $S_1$  is *const* (Fig. 5), just as the components  $S_2$  and  $S_3$  (the corresponding graphs are not presented here). We point out that this situation differs from the corresponding case of the circular motions of a spinning particle that are not highly relativistic. Indeed, then the nonzero radial spin component is not *const* but oscillates with the period of the particle's revolution by  $\varphi$ . Besides, in the last case the mean level of  $\theta$  coincides with  $90^\circ$ , whereas in Figs. 3, 8 the mean values of  $\theta$  are above  $90^\circ$ . According to Figs.

3, 8 the amplitude of the  $\theta$ -oscillation increases with the inclination angle. However,  $\theta - 90^\circ$  is small even for the inclination angle that is equal to  $90^\circ$ .

In the context of Figs. 3, 8 we point out an interesting analytical result following from Eqs. (39)–(41). Namely, it is not difficult to check that these equations are satisfied if

$$\begin{aligned}
 y_1 &= \frac{3}{1 - \delta_1}, & y_2 &= \arccos \delta_2, & y_3 &= 0, & y_4 &= 0, \\
 y_5 &= 0, & y_6 &= 0, & y_7 &= \pm \frac{1}{3\sqrt{6\delta_1}}(1 - \delta_1)^{3/2}(1 - \delta_2^2)^{-1/2}, \\
 y_8 &= \left(1 - \frac{2}{y_1}\right)^{-1/2} \sqrt{1 + y_1^2 y_7^2 (1 - \delta_2^2)}, \\
 y_9 &= \pm \frac{3\delta_2}{\sqrt{6\delta_1}}(1 - \delta_1)^{-3/2}(1 - \delta_2^2)^{-1/2}, \\
 y_{10} &= -y_9 \frac{3\delta_1}{\delta_2}(1 - \delta_1)^{-1}(1 - \delta_2^2)^{1/2}, & y_{11} &= 0, \quad (43)
 \end{aligned}$$

where  $\delta_1$  and  $\delta_2$  are some small constant values such that  $0 < \delta_1 \ll 1$ ,  $0 < |\delta_2| \ll 1$ . According to Eq. (41) the relationship between  $\delta_1$ ,  $\delta_2$  and  $\varepsilon$  from Eq. (6) is as follows:

$$\varepsilon^2 = 3\delta_1^2 + \delta_2^2. \quad (44)$$

By notation (37) we conclude that the partial solution of Eqs. (39)–(40), that is presented in Eq. (43), describes the highly relativistic nonequatorial circular motion with  $r = 3M(1 - \delta_1)^{-1}$ ,  $\cos \theta = \delta_2$ ,  $\dot{\varphi} = \text{const}$ ,  $S_1 = \text{const} \neq 0$ ,  $S_2 = \text{const} \neq 0$ ,  $S_3 = 0$ . That is, Eq. (43) shows the possibility of the spinning particle solution that orbit permanently above or below the equatorial plane, however, with the small value  $|\theta - 90^\circ|$  only. One can verify that due to the small values  $\delta_1$ ,  $\delta_2$  solution (43) is an approximate solution of the rigorous MPD equations.

Just as in the case of Schwarzschild's field, the set of Eqs. (39) with the corresponding expressions for  $A_i$  can be integrated numerically in Kerr's field. Fig. 10, as an analogy of Fig. 2, shows the plots of  $r(s)$  for some values of the inclination angle at  $a = M$ . Fig. 11 shows the dependence of the amplitude and period of the  $\theta$ -oscillation on the Kerr parameter  $a$ . The main features of Figs. 4–9 are peculiar to the corresponding plots for Kerr's field, that are not presented here for brevity.

According to Figs. 2, 6, 10 when the inclination angle is equal to  $90^\circ$ , i.e., when spin lies in the equatorial plane, so that spin-gravity coupling is equal to 0, the corresponding plots coincide with the geodesics. It is an evidence of the correct transition from solutions of the MPD equations to geodesics.

Fig. 12 illustrates some typical cases of the equatorial motions of a particle with fixed initial values of its coordinates and velocity but with different absolute value of

spin (the inclination angle is equal to  $0^\circ$ ) in Kerr's field at  $a = M$ . All curves start from  $r = 4M$  with zero radial velocity and the tangential velocity which at  $\varepsilon_0 = 10^{-4}$  is needed for the circular motion with  $r = 4M$ . This circular motion is shown by the horizontal line, whereas other curves represent the noncircular motions at  $\varepsilon_0 < 10^{-4}$  with the same particle's initial values of coordinates and velocity. According to Fig. 12 the circular orbit of a spinning particle with  $r = 4M$  monotonically trend to the corresponding noncircular geodesic orbit if  $\varepsilon_0$  trend to 0, i.e., the limiting transition  $\varepsilon_0 \rightarrow 0$  is correct.

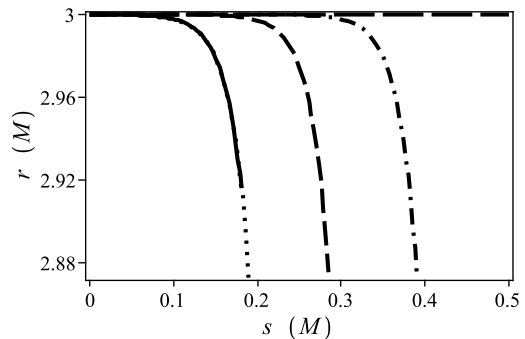


FIG. 2. Radial coordinate vs. proper time for the inclination angle  $0^\circ$  (horizontal line  $r = 3M$ ),  $1^\circ$  (dash and dot line),  $10^\circ$  (dash line), and  $90^\circ$  (solid line) at  $a = 0$ ,  $\varepsilon_0 = 10^{-4}$ . The dot line corresponds to the geodesic motion with the same initial values of the coordinates and velocity.

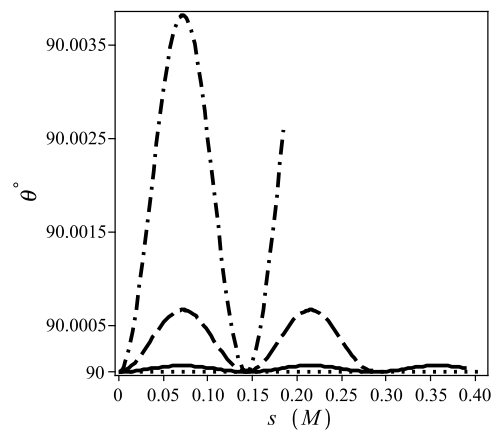


FIG. 3. Graphs of the angle  $\theta$  vs. proper time for the inclination angle  $0^\circ$  (horizontal line  $\theta = 90^\circ$ ),  $1^\circ$  (solid line),  $10^\circ$  (dash line), and  $90^\circ$  (dash and dot line) at  $a = 0$ ,  $\varepsilon_0 = 10^{-4}$ .

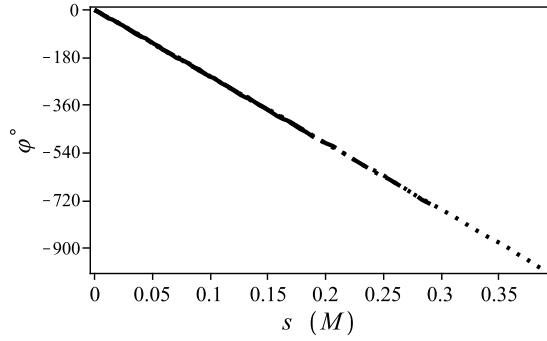


FIG. 4. Graphs of the angle  $\varphi$  vs. proper time at  $a = 0$ ,  $\varepsilon_0 = 10^{-4}$  for different values of the inclination angle practically coincide with the corresponding geodesic plot. The same feature takes place for the corresponding graphs  $t$  vs.  $s$  that are not presented here for brevity.

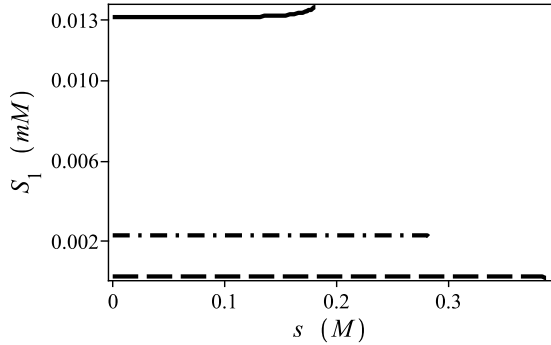


FIG. 5. Graphs of  $S_1$  vs. proper time for the inclination angle  $1^\circ$  (dash line),  $10^\circ$  (dash and dot line), and  $90^\circ$  (solid line) at  $a = 0$ ,  $\varepsilon_0 = 10^{-4}$ .

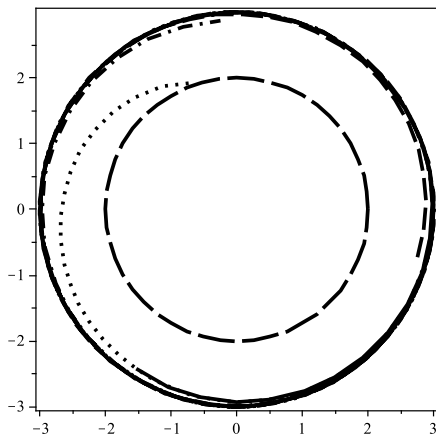


FIG. 6. Trajectories of the spinning particle in the polar coordinates for the inclination angle  $0^\circ$  (circle  $r = 3M$ ),  $1^\circ$  (dash line),  $10^\circ$  (dash and dot line), and  $90^\circ$  (solid line) at  $a = 0$ ,  $\varepsilon_0 = 10^{-4}$ . The dot line corresponds to the geodesic motion with the same initial values of the coordinates and velocity. The circle  $r = 2M$  corresponds to the horizon line.

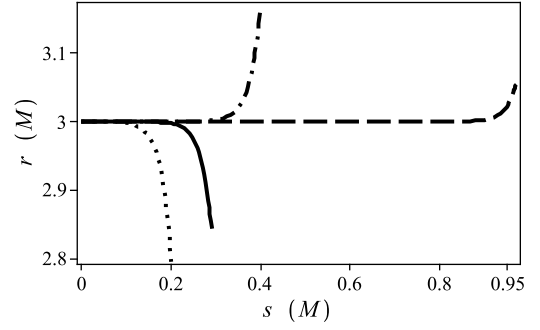


FIG. 7. Radial coordinate vs. proper time for the inclination angle  $0^\circ$  (dash and dot line),  $1^\circ$  (dash line), and  $10^\circ$  (solid line) at  $a = 0$ ,  $\varepsilon_0 = 10^{-4}$ , and the nonzero radial velocity  $dr/ds \approx 3.858 \times 10^{-7}$ . The dot line corresponds to the geodesic motion with the same initial values of the coordinates and velocity.

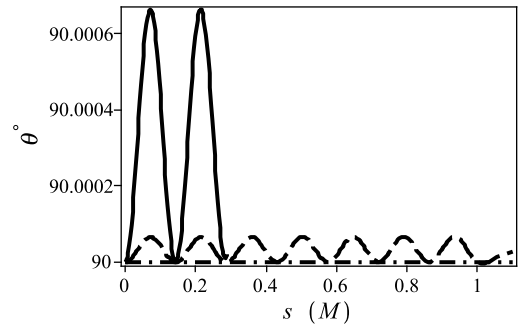


FIG. 8. Graphs of the angle  $\theta$  vs. proper time for the inclination angle  $0^\circ$  (horizontal line),  $1^\circ$  (dash line) and  $10^\circ$  (solid line), at  $a = 0$ ,  $\varepsilon_0 = 10^{-4}$ , and  $dr/ds \approx 3.858 \times 10^{-7}$ .

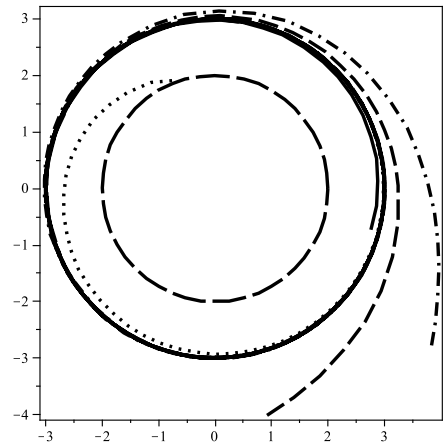


FIG. 9. Trajectories of the spinning particle in the polar coordinates for the inclination angle  $0^\circ$  (dash and dot line),  $1^\circ$  (dash line), and  $10^\circ$  (solid line) at  $a = 0$ ,  $\varepsilon_0 = 10^{-4}$ , and  $dr/ds \approx 3.858 \times 10^{-7}$ . The dot line corresponds to the geodesic motion with the same initial values of the coordinates and velocity.

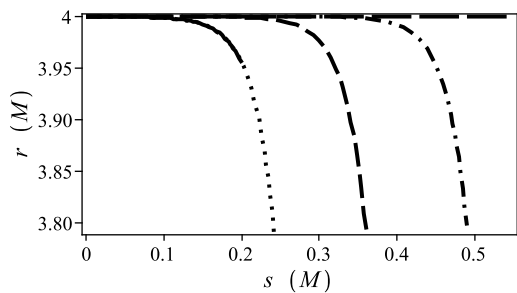


FIG. 10. Radial coordinate vs. proper time for the inclination angle  $0^\circ$  (horizontal line  $r = 4M$ ),  $1^\circ$  (dash and dot line),  $10^\circ$  (dash line), and  $90^\circ$  (solid line) at  $a = M$ ,  $\varepsilon_0 = 10^{-4}$ . The dot line corresponds to the geodesic motion with the same initial values of the coordinates and velocity.

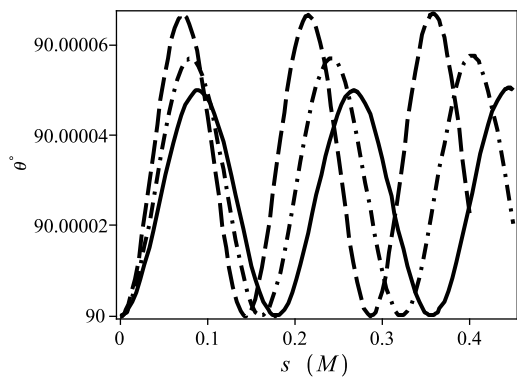


FIG. 11. Graphs of the angle  $\theta$  vs. proper time for the inclination angle  $1^\circ$  at  $a = 0$  (dash line),  $a = 0.5M$  (dash and dot line),  $a = M$  (solid line);  $\varepsilon_0 = 10^{-4}$ .

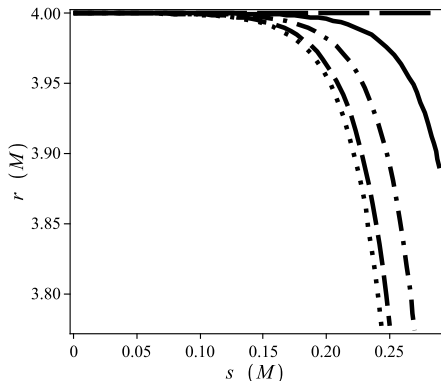


FIG. 12. Radial coordinate vs. proper time for the equatorial motions in Kerr's field at  $a = M$  with different absolute value of spin and the same (common) initial values of the coordinates and velocity. The circular orbit with  $r = 4M$  at  $\varepsilon_0 = 10^{-4}$  is shown by the long dash line. The solid, dash and dot, and dash lines describe the cases when  $\varepsilon_0$  is equal to  $0.9 \times 10^{-4}$ ,  $0.6 \times 10^{-4}$ , and  $0.2 \times 10^{-4}$  correspondingly. The dot line represents the geodesic motion with the same initial values of the coordinates and velocity.

Finally, we remark on a simple conclusion following from the nongeodesic curves of a spinning particle presented, in part, in Figs. 2–12. Let us consider any point on the trajectory of a spinning particle corresponding to its proper time  $s_1 > 0$  (we recall that all curves in Figs. 2–12 begin at  $s = 0$ ). Then the geodesic curve can be calculated which starts just at this point with the velocity that is equal to the velocity of the spinning particle at the same point. Also, it is not difficult to estimate the deviation of the pointed out nongeodesic curve from this geodesic. In principle, it means that in our comparison of the corresponding geodesic and nongeodesic curves we are not restricted to the trajectories of a spinning particle which start in the small neighborhood of the value  $r = r_{ph}^{(-)}$  only (naturally, here we are restricted to the domain of validity of the linear spin approximation). This conclusion may be useful for the generalization of the results obtained in this Sec. on other motions of a spinning particle.

## V. CONCLUSIONS

In this paper, using the linear spin approximation of the MPD equations, we have studied the significantly nongeodesic highly relativistic motions of a spinning particles starting near  $r = r_{ph}^{(-)}$  in Kerr's field. Some of these motions, namely circular, are described by the analytical relationships following directly from MPD equations in the Boyer-Lindquist coordinates. Others, noncircular and nonequatorial, are calculated numerically. For realization of these motions the spinning particle must possess the orbital velocity corresponding to the relativistic Lorentz  $\gamma$ -factor of order  $1/\sqrt{\varepsilon}$ . All considered cases of the spinning particle motion are within the framework of the validity of the test-particle approximation when  $\varepsilon \ll 1$ .

The situation with a macroscopic test particle moving relative to a massive body with  $\gamma^2 \gg 1$  is not realistic. However, the highly relativistic values of the Lorentz  $\gamma$ -factor are usual in astrophysics for the elementary particles. For example, if  $M$  is equal to three of the Sun's mass (as for a black hole), then  $\varepsilon_0$  for an electron is of order  $0.4 \times 10^{-16}$  and from Eq. (28) we have the  $\gamma$ -factor of order  $2 \times 10^8$ . Similarly, for a neutrino with the mass  $\approx 1eV$  we have  $\varepsilon_0 \approx 2 \times 10^{-11}$ ,  $\gamma \approx 3 \times 10^5$ .

We can expect the effects of the significant space separation of some highly relativistic particles with different orientation of spin. Indeed, the effects considered in this paper exhibit the strong repulsive action of the spin-gravity interaction. For another correlation of signs of the spin and the particle's orbital velocity this interactions acts as an attractive force. In general, the last case is beyond the validity of the linear spin approximation. The nonlinear spin effects will be investigated in another paper. Also, we plan to show that according to the MPD equations significantly nongeodesic orbits of a highly relativistic spinning particle, with the  $\gamma$ -factor of order  $1/\sqrt{\varepsilon}$ , exist for the much wider space region of the initial val-

ues of the particle's coordinates in a Kerr spacetime than the orbits considered above. However, the corresponding calculations are very complicated because this result follows from the rigorous MPD equations (1), (2) only, and

is not common for the approximate equations (2), (7).

Naturally, it would be interesting to study the possible role of the highly relativistic spin-gravity interaction in the jet formation.

- 
- [1] L. D. Landau and E. M. Lifshitz, *The classical theory of fields* (Addison-Wesley, Reading, Massachusetts, 1971).
- [2] C. W. Misner, K. S. Thorne, and J. A. Wheeler, *Gravitation* (Freeman, San Francisco, 1973).
- [3] S. Chandrasekhar, *The Mathematical Theory of Black Holes* (Oxford University Press, Oxford, 1983).
- [4] J. Gariel, M. A. H. MacCallum, G. Marcilhacy, and N. O. Santos, *Astron. and Astrophys.* **515**, A15 (2010).
- [5] M. Banados, J. Silk, and S. M. West, *Phys. Rev. Lett.* **103**, 111102 (2009); E. Berti, V. Cardoso, L. Gualtieri, F. Pretorios, and U. Sperhake, *Phys. Rev. Lett.* **103**, 239001 (2009); T. Jacobson and T. Sotiriou, *Phys. Rev. Lett.* **104**, 021101 (2010).
- [6] E. Hackmann, V. Kagramanova, J. Kunz, and C. Lämmerzahl, *Europhys. Lett.* **88**, 30008 (2009).
- [7] M. Mathisson, *Acta Phys. Polon.* **6**, 163 (1937).
- [8] A. Papapetrou, *Proc. R. Soc. A* **209**, 248 (1951).
- [9] W. G. Dixon, *Proc. R. Soc. A* **314**, 499 (1970); *Gen. Relativ. Gravitation* **4**, 199 (1973); *Philos. Trans. R. Soc. A* **277**, 59 (1974); *Acta Phys. Pol. B. Proc. Suppl.* **1**, 27 (2008).
- [10] R. Wald, *Phys. Rev. D* **6**, 406 (1972).
- [11] W. Tulczyjew, *Acta Phys. Pol.* **18**, 393 (1959); A. Taub, *J. Math. Phys.* **5**, 112 (1964); P. Bartrum, *Proc. R. Soc. A* **284**, 204 (1965); H. P. Künzli, *J. Math. Phys.* **13**, 739 (1972); M. Omote, *Progr. Theor. Phys.* **49** 1559 (1973); S. Hojman, *Phys. Rev. D* **18**, 2741 (1978); A. Balachandran, G. Marmo, B. Skagerstam, and A. Stern, *Phys. Lett. B* **89** 199 (1980).
- [12] J. Natario, *Commun. Math. Phys.* **281**, 387 (2008); E. Barausse, E. Racine, and A. Buonanno, *Phys. Rev. D* **80**, 104025 (2009); J. Steinhoff and G. Schäfer, *Europhys. Lett.* **87**, 50004 (2009).
- [13] B. M. Barker and R. F. O'Connell, *Gen. Rel. Grav.* **4**, 193 (1973).
- [14] A. N. Aleksandrov, *Kinem. Fiz. Nebesn. Tel.* **7**, 13 (1991).
- [15] B. Mashhoon, *J. Math. Phys.* **12**, 1075 (1971).
- [16] K. P. Tod, F. de Felice, and M. Calvani, *Nuovo Cim. B* **34**, 365 (1976).
- [17] S. Suzuki and K. Maeda, *Phys. Rev. D* **58**, 023005 (1998).
- [18] O. Semerak, *Mon. Not. R. Astron. Soc.* **308**, 863 (1999).
- [19] M. Hartl, *Phys. Rev. D* **67**, 024005 (2003); *Phys. Rev. D* **67**, 104023 (2003).
- [20] C. Chicone, B. Mashhoon, and B. Punsly, *Phys. Lett. A* **343**, 1 (2005).
- [21] B. Mashhoon and D. Singh, *Phys. Rev. D* **74**, 124006 (2006).
- [22] D. Singh, *Phys. Rev. D* **78**, 104028 (2008).
- [23] R. Plyatsko, *Phys. Rev. D* **58**, 084031 (1998).
- [24] R. Plyatsko and O. Bilaniuk, *Class. Quantum Grav.* **18**, 5187 (2001).
- [25] R. Plyatsko, *Class. Quantum Grav.* **22**, 1545 (2005).
- [26] S. Wong, *Int. J. Theor. Phys.* **5**, 221 (1972); L. Kanenberg, *Ann. Phys. (N.Y.)* **103**, 64 (1977); R. Catenacci and M. Martellini, *Lett. Nuovo Cimento* **20**, 282 (1977); J. Audretsch, *J. Phys. A* **14**, 411 (1981); A. Gorbatsievich, *Acta Phys. Pol. B* **17**, 111 (1986); A. Barut and M. Pavsic, *Class. Quantum Grav.* **4**, 41 (1987).
- [27] F. Cianfrani and G. Montani, *Europhys. Lett.* **84**, 30008 (2008); *Int. J. Mod. Phys. A* **23**, 1274 (2008); Yu. Obukhov, A. Silenko, and O. Teryaev, *Phys. Rev. D* **80**, 064044 (2009).
- [28] R. Micoulaut, *Z. Phys.* **206**, 394 (1967).